Lévy Curves

Kelsey Bates

June 8, 2015

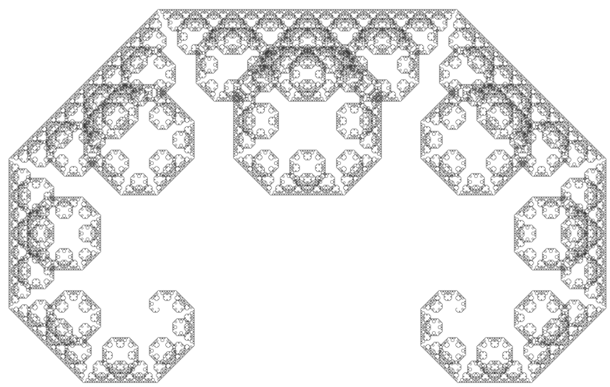

Figure 1: A Lévy curve

Contents

1 Introduction

The Lévy curve, or Lévy dragon, is a recursive fractal with some very interesting properties, as shown in Scott Bailey, Theodore Kim, and Robert S. Strichartz's paper "Inside the Lévy Dragon" [1]. It was named for Paul Lévy in the early 20th century, [1, p. 689] and is still one of the more recognizable fractals. While its construction may seem simple at first, we will find it is more interesting and complicated than one might expect.

We will begin by constructing the curve itself and a useful approximation using triangles. Next we will apply these to discover and investigate many of the interesting shapes found within the Lévy curve. We will end with an overview of the similarities and differences between the Lévy curve and the closely related dragon curve, including a brief discussion of how we might apply the ideas in Sections 2 and 3 to the dragon curve.

2 Constructing the Lévy Curve

2.1 Usual Construction

The Lévy curve is usually constructed with lines. We begin with a single straight line, and for each successive step we replace each line with an angle of $\pi/2$. [2, p. 46] The first few steps of this are shown in Figure 2. The Lévy curve D is the curve formed when this process is repeated infinitely, or when $m \to \infty$. We can show that the Lévy curve has infinite length. If we let the length of the original line segment be 1, then the length of a given segment in the mth step is $2^{-m/2}$ and there are 2^m such lines. We see that

$$\lim_{m\to\infty} 2^{-m/2} \cdot 2^m = \lim_{m\to\infty} 2^{m/2} = \infty.$$

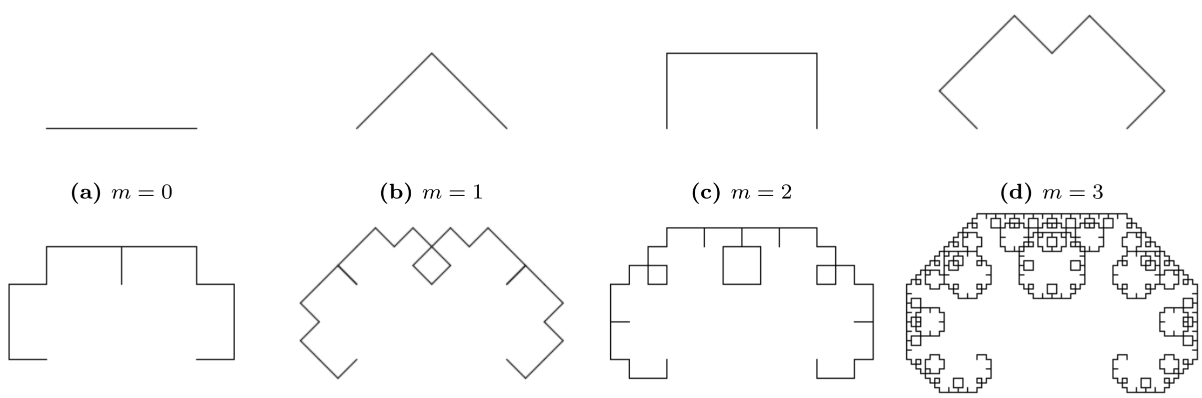

(a) $m = 0$ **(b)** $m = 1$ **(c)** $m = 2$ **(d)** $m = 3$

(e) $m = 4$ **(f)** $m = 5$ **(g)** $m = 6$ **(h)** $m = 10$

Figure 2: Usual Lévy curve construction

Later on we will be discussing the interior of D. However, a curve cannot have an interior by the standard definition. We will let D' be the set of all points $\mathbf{x}$ such that for all $\varepsilon > 0$, there exists an M such that the disk of radius ε about $\mathbf{x}$ contains a point in D_m for $m > M$. More intuitively, D' is the set of points that are arbitrarily close to D. We will redefine the interior of D as the interior of D'.

2.2 A Convenient Approximation

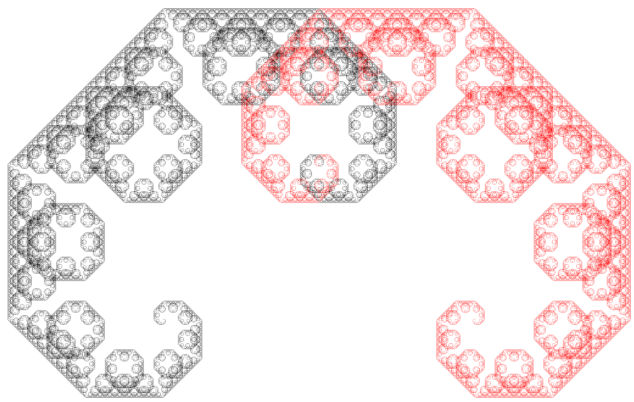

Figure 3: The Lévy curve is made up of two identical but smaller curves

We will approximate the Lévy curve by taking advantage of the its self-similarity. Note in Figure 3 that one curve D is made by combining two curves under the transformations F_1 and F_2. Both F_1 and F_2 scale D down by $1/\sqrt{2}$, and F_1 rotates D by $\pi/4$ while F_2 rotates D by $-\pi/4$. Symbolically we can write [1, p. 690]

$$D = F_1 D \cup F_2 D. \tag{1}$$

If we take the area of D (meaning the area of its interior) to be 1, then the areas of $F_1 D$ and $F_1 D$ must each be $(1/\sqrt{2})^2 = 1/2$. Since $2 \cdot 1/2 = 1$, we see that the interiors of $F_1 D$ and $F_2 D$ must not overlap, even though the curves obviously intersect. [1, p. 690]

Thus we can recursively generate an approximation of the Lévy curve. We will let D_0 be some arbitrary shape. Then we will define

$$D_m = F_1 D_{m-1} \cup F_2 D_{m-1}. \tag{2}$$

D_0 can be any shape (see Figure 4) since as $m \to \infty$, the size of the shape will become very small and insignificant. However, for the purposes of this paper, we will find it useful to use a right isosceles triangle T. The details of this are shown in Figure 5. It is important to remember that our approximations are just that: approximations. However, by [1, pg. 692], these approximations should be accurate for length scales greater than $2^{-m/2}$.

There is another way to interpret this. We start out with T (refer to Figure 5). To get to D_1, instead of scaling and rotating, we can picture dividing T down the center to create two

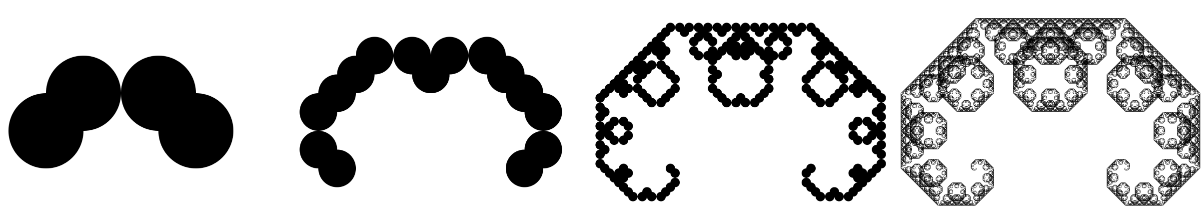

(a) $m = 2$ **(b)** $m = 4$ **(c)** $m = 8$ **(d)** $m = 18$

Figure 4: Constructing Lévy curve approximations from circles

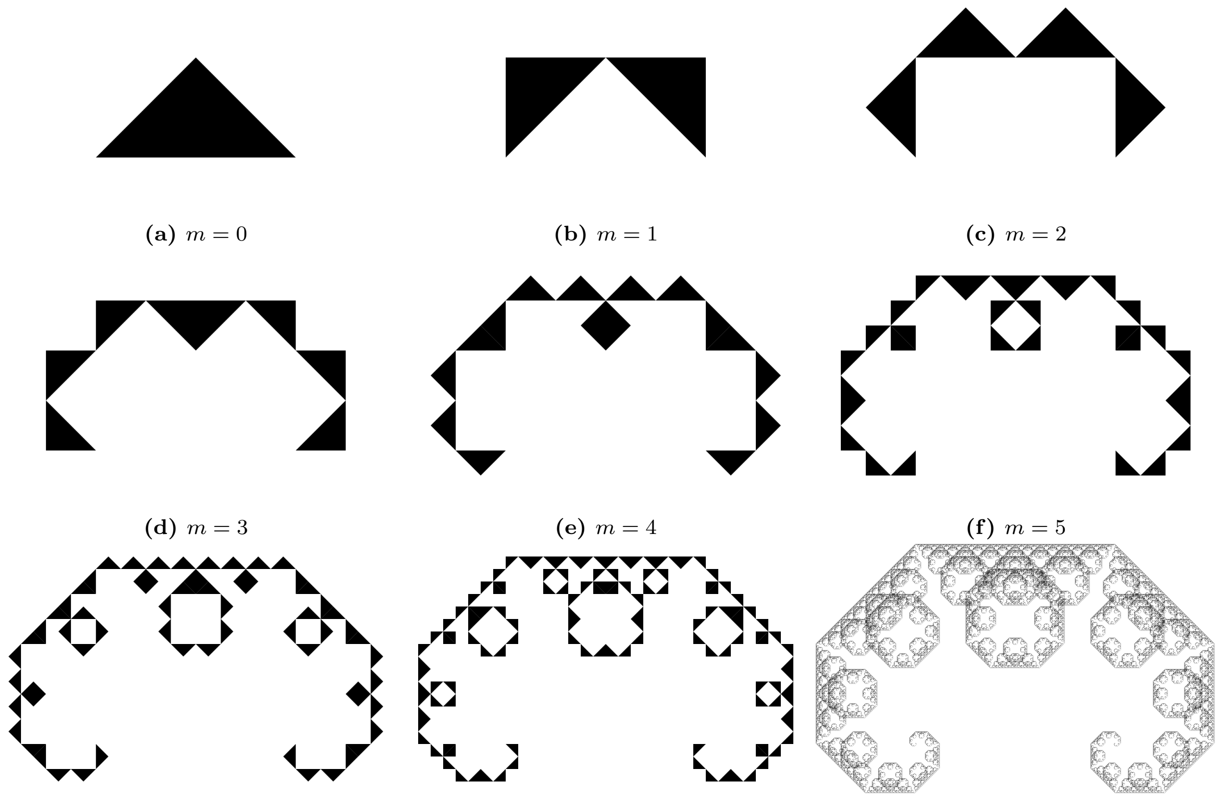

(a) $m = 0$ **(b)** $m = 1$ **(c)** $m = 2$

(d) $m = 3$ **(e)** $m = 4$ **(f)** $m = 5$

(g) $m = 6$ **(h)** $m = 7$ **(i)** $m = 20$

Figure 5: Constructing Lévy curve approximations from T

smaller right triangles. Note that these are similar to T, since they have the same angles, and are scaled down by $1/\sqrt{2}$, since what was a side length is now the hypotenuse. Then we reflect each of these triangles across their respective hypotenuses and finally arrive at D_1. Next we continue by performing the same process on each of the triangles in D_m to get D_{m+1}. By this method, it is easy to see that $\text{Area}\,(D_m) = \text{Area}(T)$ for all $m \geq 0$. However, it is important to note that $\text{Area}\,(D_m)$ does not necessarily equal $\text{Area}(D)$ since D_m is only an approximation of D.

2.3 Tesselating

The reason we chose T above is because of its ability to tesselate over $\mathbb{R}^2$ as seen in Figure 6. We will call this pattern G and write (g refers to a specific position in G), [1, p. 691]

$$\bigcup_{g \in G} gT = \mathbb{R}^2. \tag{3}$$

Proposition 1. *D_m tesselates by the process G over $\mathbb{R}^2$, or* [1, p. 691]

$$\bigcup_{g \in G} gD_m = \mathbb{R}^2. \tag{4}$$

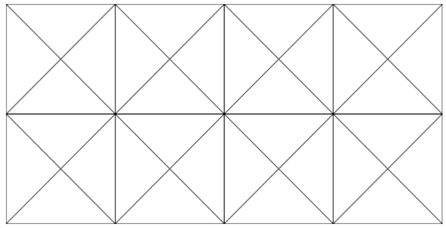

Figure 6: Tesselating T

Proof. We will prove this inductively using the interpretation at the end of the previous section.

For the base case, $D_0 = T$, so we know it tesselates (see Figure 6).

We will assume that D_m tesselates by G, and prove that D_{m+1} tesselates by G. We know that D_m is made up of triangles similar to T, which therefore must tesselate as shown in Figure 6. To get D_{m+1}, we begin by dividing each triangle down the center (the red lines in Figure 7). Next we would need to reflect each smaller triangle across its hypotenuse. As can be seen in the figure, this essentially means each triangle will switch places with its neighbor along its hypotenuse. Thus in D_{m+1}, no two triangles overlap. As shown in the previous section, the areas of D_m and D_{m+1} are equal, thus D_{m+1} tesselates and covers $\mathbb{R}^2$. □

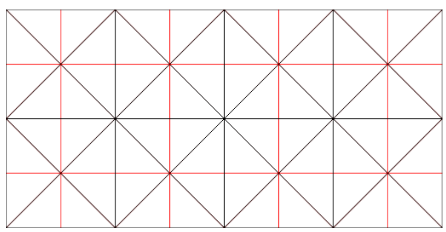

Figure 7: Proving D_{m+1} tesselates. The red lines divide the triangles in Figure 6 in half.

It is difficult to show these tesselations since the Lévy curves cross each other, but the interactions between four curve approximations are shown in Figure 8. This arrangement is also somtimes called Lévy's Tapestry [2, p. 47]. Figure 21 in Appendix B contains a tesselation of D_{20} curve approximations as well.

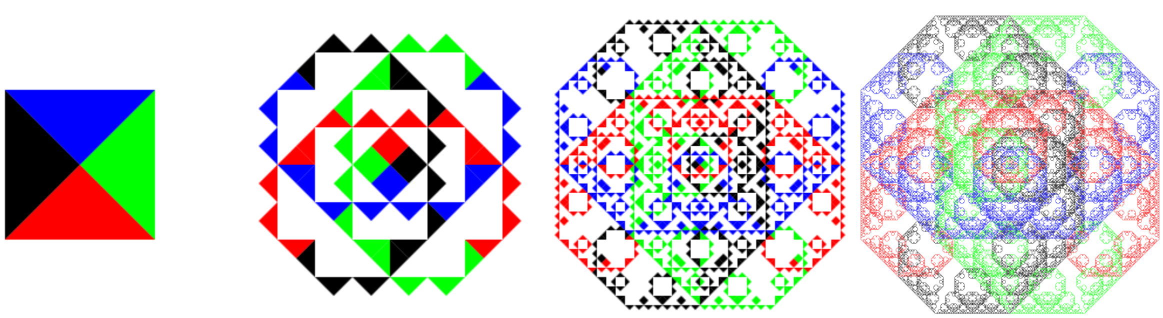

(a) $m = 0$ **(b)** $m = 4$ **(c)** $m = 8$ **(d)** $m = 14$

Figure 8: Four interacting Lévy curve approximations

3 The Interior of a Lévy Curve

3.1 Finding the Interior

Now we can use our approximations to find regions in the interior of D.

Proposition 2. *The interior of a triangle T' in D_m is contained in D if the 15 triangles shown in Figure 9 (including T') are contained in D_m. Note that these are all the triangles which share at least one boundary point with the center triangle.* [1, p. 692]

Proof. [1, p. 692] For D, each triangle in D_m will be replaced by Lévy curves. In the figure, the Lévy curve made from T' (the shaded triangle) is shown in red. Notice how it is completely contained in the fifteen triangles (this could be shown using the method to construct approximations at the end of Section 2.2). Also notice that it intersects T'. If we replace any of the other fourteen triangles with its corresponding Lévy curve, the curve will also intersect T'. However, if we replace any other similarly tesselated triangle with its corresponding Lévy curve, the curve will not intersect T' (except possibly on the boundary).

Recall Proposition 1, so tesselations of Lévy curves cover $\mathbb{R}^2$. Thus, since all tesselated Lévy curves which could intersect the interior of shaded triangle do so, the interior of central triangle must be contained in D. □

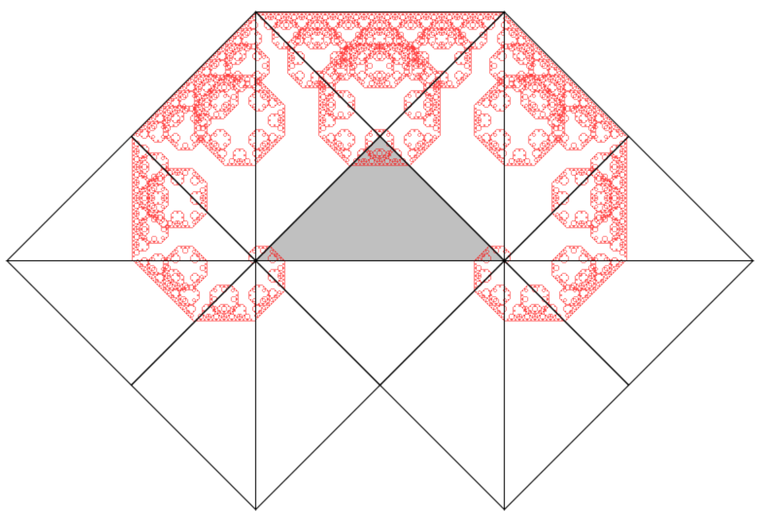

Figure 9: The fifteen triangles bordering the center shaded triangle, T', with a Lévy curve made from the shaded triangle in the background.

We will say triagles satisfying this property for D_m are in $(D_m)^{\text{int}}$. We will use an example to illustrate how this works. The first nonempty $(D_m)^{\text{int}}$ is at $m = 14$. [1, p. 693]. Figure 10 (a) shows this region (highlighted in green and later blue, see caption). As m increases, the region gets larger until $m = 16$, where it reaches its maximum size. We can compare its size to that of $m = 27$ (which is reasonably close to D at this scale). We know from Proposition 2 that this region is contained in D. These images suggest that the boundary of this region (for $m \geq 16$) is the boundary of a region in D. This leads us to the Border Algorithm.

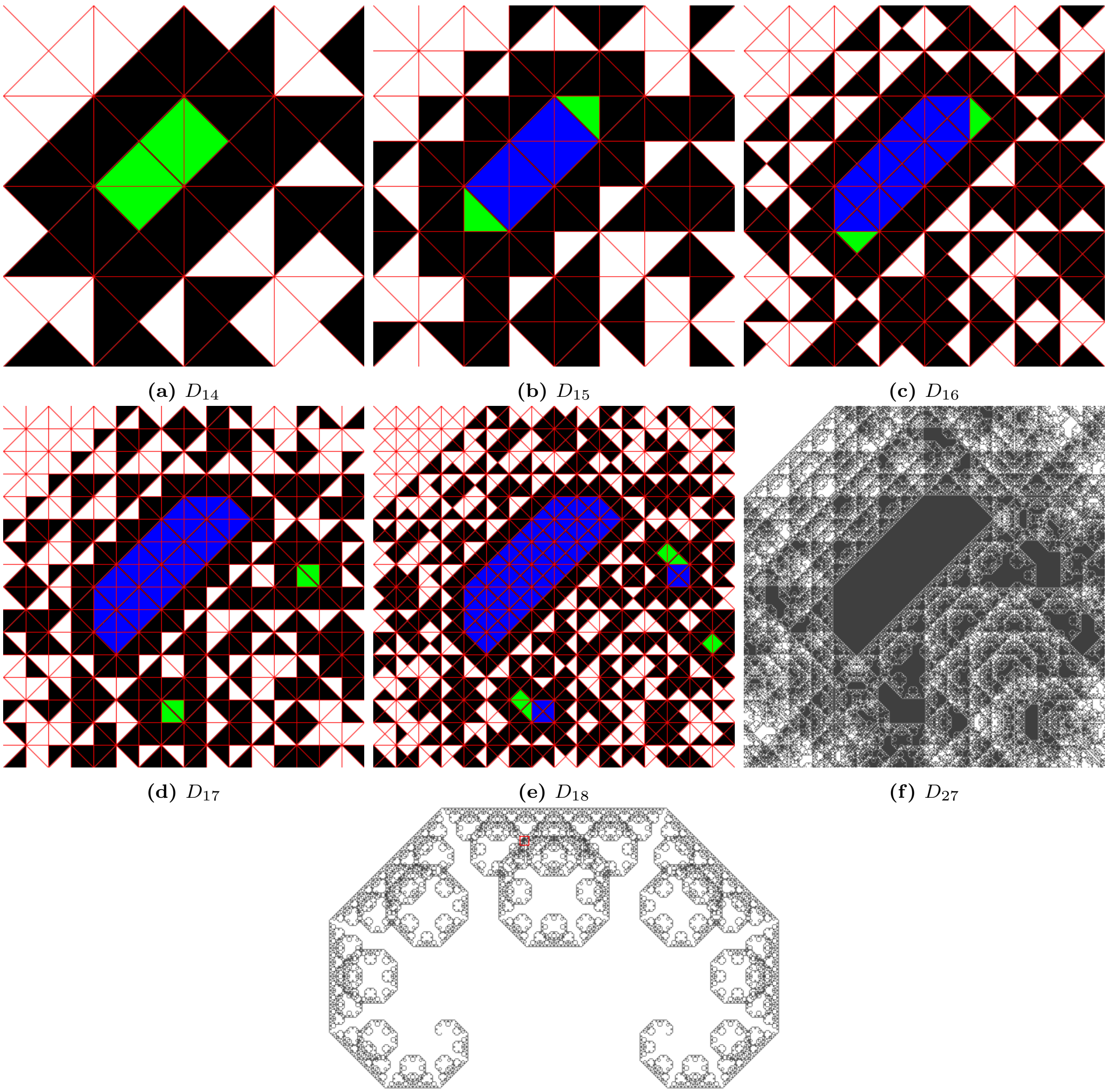

(a) D_{14} **(b)** D_{15} **(c)** D_{16}

(d) D_{17} **(e)** D_{18} **(f)** D_{27}

(g) The red border outlines the magnified portion

Figure 10: Applying Proposition 2 to a portion of D_m. The blue and green represent triangles in $(D_m)^{\text{int}}$ and the green specifically reprents those triangles not in $(D_{m-1})^{\text{int}}$.

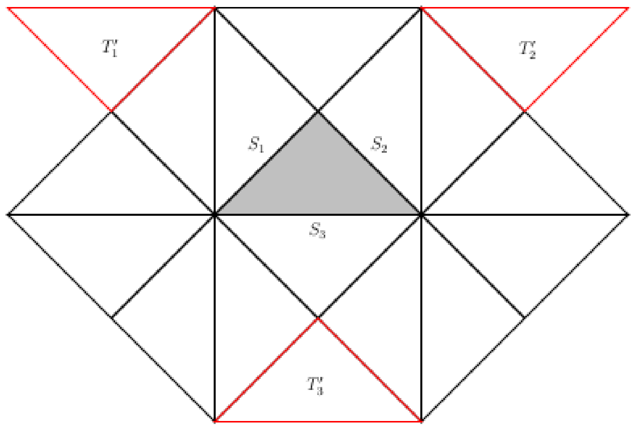

Figure 11: The fifteen triangles bordering the center shaded triangle (T'), and the three control triangles.

Border Algorithm. *Let T' be a triangle such that $T' \subset (D_m)^{\text{int}}$ but $T' \not\subset (D_{m-1})^{\text{int}}$. For each side S_j of T' there is a control triangle T_j' (see Figure 11) such that:* [1, p. 695]

- *If $T_j' \not\subset D_m$, then S_j belongs to the boundary of a figure in D.*
- *If $T_j' \subset D_m$, then S_j does not belong to the boundary of a figure in D (excluding endpoints).*

Proof. [1, pp. 695-697] First we will assume $T_j' \not\subset D_m$ (it does not matter whether $T' \not\subset (D_{m-1})^{\text{int}}$). D_{m+1} is depicted in Figure 12b, where only blue trianges are in D_{m+1}. Thus we can visually see that for D_{m+1}, S_j will have a new triangle (or for S_3, two new triangles) that is both closer than T_j' and not in D_{m+1}. Since the conditions for S_j for both D_m and D_{m+1} are identical, we can infer by induction that for any disk centered on the side there will always be an M such that the disk contains a point not in D_m when $m > M$. This disk must also contain a point in D_m since it must contain a point in T'. Thus the point is a boundary point.

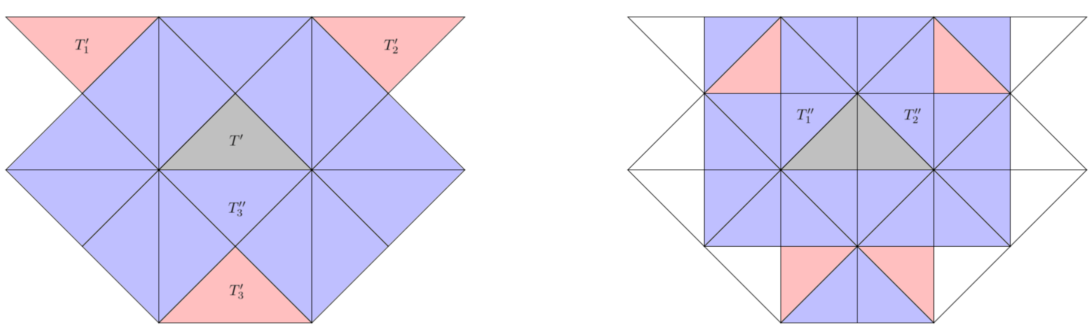

(a) D_m

(b) D_{m+1}

Figure 12: Red triangles correspond to T_1', T_2', and T_3' in D_m and their correspnding triangles in D_{m+1}. Blue triangles correspond to those bordering T' in D_m and their corresponding triangles in D_{m+1}. Figure 12b is made by following the process at the end of Section 2.2.

Next we will assume $T_j' \subset D_m$ (in Figure 12 both the blue triangles and the red triangles corresponding to T_j are in D_m and D_{m+1}). We see that T_3'', as defined in Figure 12a, must be in D by Proposition 2. Thus, since S_3 (excluding endpoints) is surrounded by T' and T_3'', which are both in D, it cannot belong to the boundary of D. Note that this means as we increase m, $(D_m)^{\text{int}}$ can only "grow" along the short sides of triangles.

Finally we will assume $T_j' \subset D_m$ and look at S_1 and T_1, and S_2 and T_2. Since these cases are symmetrical, we only need to look at S_1 and T_1. This time we must go to D_{m+1}. Again we see that T_1'', as defined in Figure 12b, must be in D, by Proposition 2. Thus, since S_1 (excluding endpoints) is surrounded by T' and T_1'', which are both in D, it cannot belong to the boundary of D. □

3.2 Shapes in the Interior

We define a shape as the largest open connected set for a section in the interior of D and its boundary. By generating D_m for large m, Bailey, Kim, and Strichartz were able to find sixteen distinct shapes (not including reflections) in the Lévy curve. [1, p. 697] However, they have not disproved the possibility of other shapes.

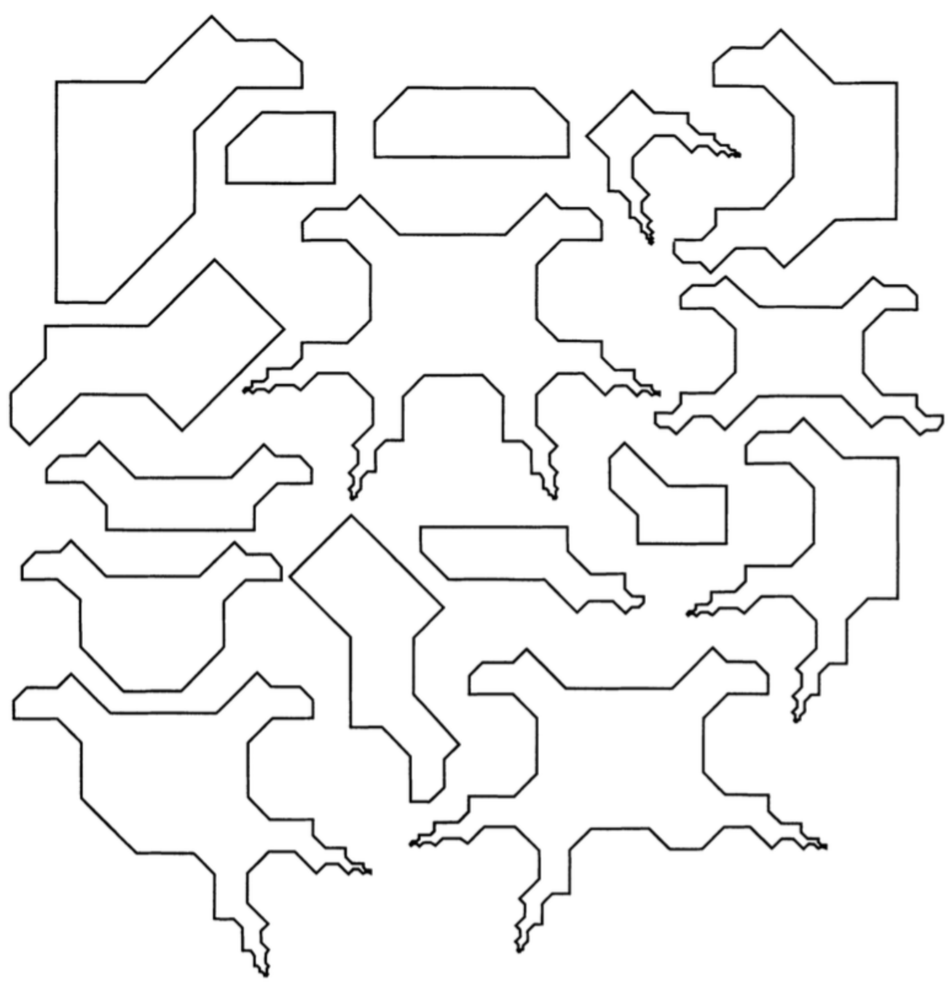

Figure 13: The sixteen distinct shapes found in D. [1, p.696]

Conjecture 1. *Every shape in D is similar to those seen in Figure 13.* [1, p. 697]

We can observe many of these shapes in Figures 22 and 23 in Appendix B. From Figure 13 we see that there are both shapes with a finite number of sides and shapes with an infinite number of sides. The shapes with an infinite number of sides have "legs", which are the pointed parts where the infinite number of sides are clustered. We can see the formation of one such leg in Figure 14. In this figure, note that from D_{24} on, each step adds on four triangles: three on the tip of the leg, and one on the edge of the addition from the previous step. This process will continue on, and an approximation of the leg of D can be seen in D_{33}. Furthermore, all legs will grow this way. [1, p. 697]

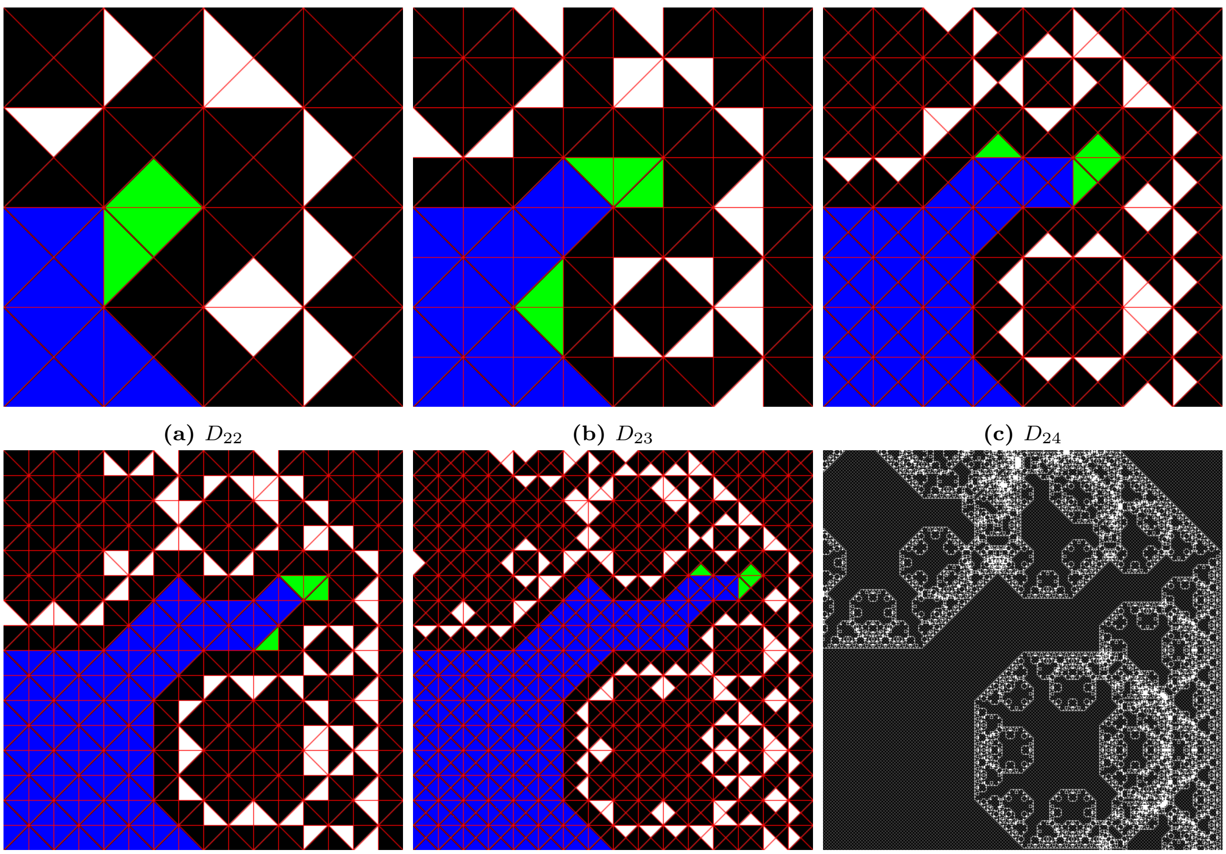

(a) D_{22} **(b)** D_{23} **(c)** D_{24} **(d)** D_{25} **(e)** D_{26} **(f)** D_{33}

Figure 14: The formation of a leg. The blue and green represent triangles in $(D_m)^{\text{int}}$ and the green specifically reprents those triangles not in $(D_{m-1})^{\text{int}}$.

The shapes depicted in Figure 13 each have anywhere from zero to four legs. There is only one four-legged shape, which we will call a "baby dragon". The baby dragon can also be seen in the white space in "loops" in the Lévy curve (see Figure 1). The baby dragon also appears to have an interesting relationship to the other shapes in D. [1, p. 697]

Conjecture 2. *Every shape in D can be made by cutting the baby dragon with a finite number of half-planes.* [1, p. 697]

We can use either of these conjectures to prove that the boundary of any shape in D is finite. We only need to prove that the boundary of a leg is finite. Say the boundary of a leg of a specific shape in D_m is B, and the boundary of this leg in D_{m+1} is $B+b$. It follows from Figure 14 that the boundary of this leg in D_{m+2} is $B+b+\frac{1}{\sqrt{2}}b$, and the boundary of this leg in D_{m+n} is $B+b\sum_0^{n-1} 2^{-n/2}$. Thus this leg in D will have length

$$B+b\sum_0^{\infty} 2^{-n/2} = B+b\sum_0^{\infty}\left(\frac{1}{\sqrt{2}}\right)^n$$

which is a convergent geometric series. There is a rigorous proof that the boundary of any shape in D is finite (so it does not rely on conjectures) in [1, p. 699].

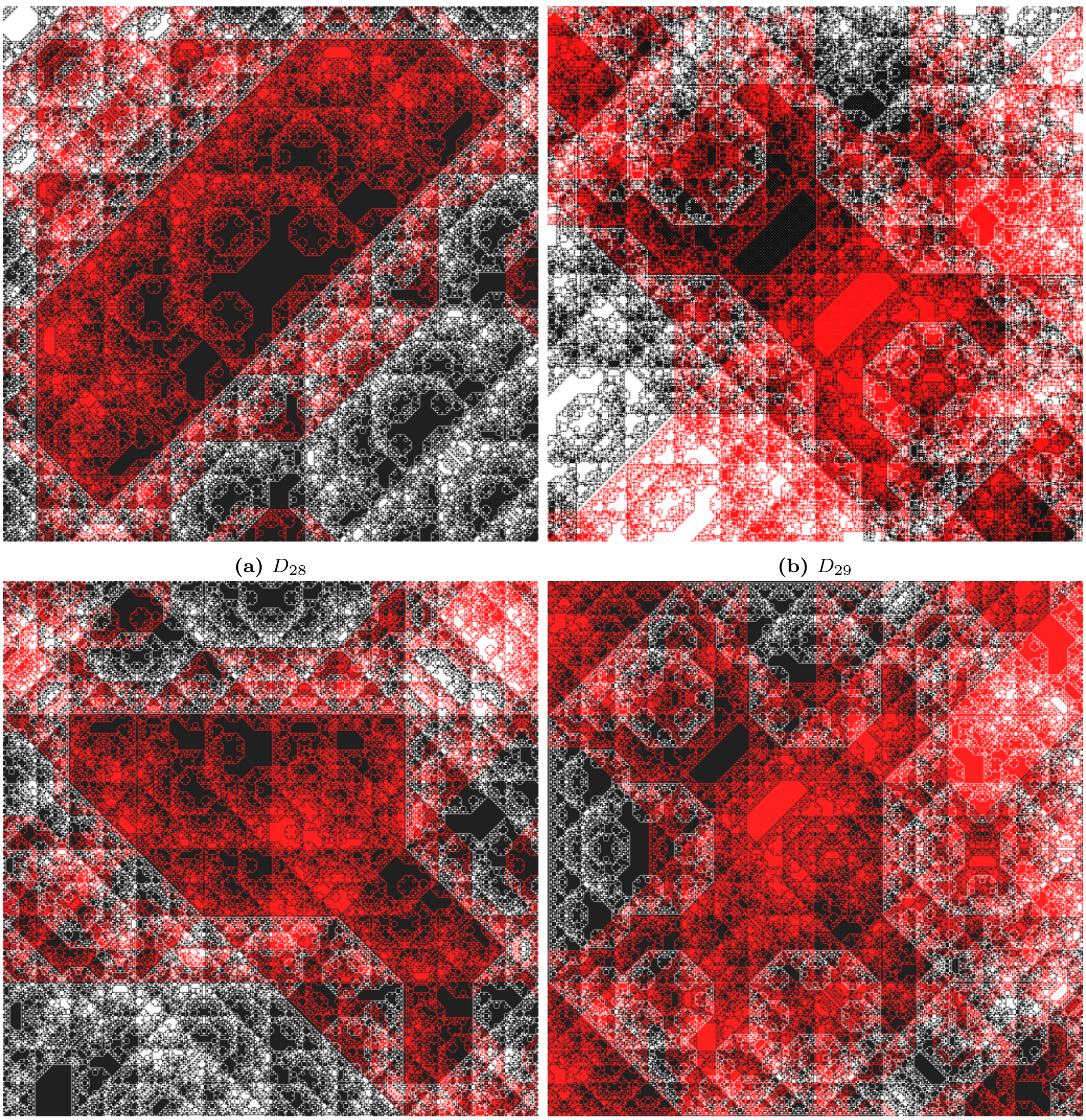

(a) D_{28} **(b)** D_{29} **(c)** D_{32} **(d)** D_{34}

Figure 15: Interacting F_1 (black) and F_2 (red)

3.3 Combining Two Curves

Recall from Equation (1) and Figure 3 that a Lévy curve can be broken down into two smaller Lévy curves. It is interesting to look at how these curves interact to form shapes in D.

Conjecture 3. *If S is a shape in D, and S^{int} overlaps both F_1 and F_2 (see Equation (1), then F_1 and F_2 each contain an infinite number of shapes in S.* [1, p. 701]

We can see examples of this in Figure 15. One thing to remember is due to Proposition 1, none of these infinite shapes overlap. From this figure we can see that there are multiple ways to form a specific shape. Take for example, the baby dragon in Figure 15d. We see that there are other smaller baby dragons in Figure 15d, but they are made up of completely different shapes. However, Bailey, Kim, and Strichartz assert that the number of possible ways to make a given shape is bounded since each is stemmed from a specific configuration of triangles for some D_m. [1, p. 702] It is also interesting to look for shapes in Figure 21 in Appendix B as different color combinations will form different shapes.

4 The Dragon Curve

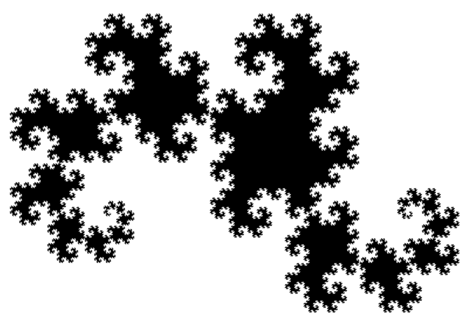

Figure 16: A dragon curve

The dragon curve (as shown in Figure 16) is very similar to the Lévy curve, but has very different properties. While its construction is usually described as the result of repeatedly folding a strip of paper [2, p. 49], we will find it easier to think abount it by modifying Equation 2. While F_1 is still a rotation by $\pi/4$, F_2 is a rotation by $3\pi/4$. If we denote these changes with asterisks, we can write

$$D_m^* = F_1 D_{m-1}^* \cup F_2^* D_{m-1}^*. \tag{5}$$

Alternatively, we can use the method at the end of Section 2.2. Instead of reflecting both triangles across their hypotenuses, we only reflect evey other one. The result is shown in Figure 17. Again, this is only an approximation because the dragon curve is also originally constructed by taking taking the limit of curves.

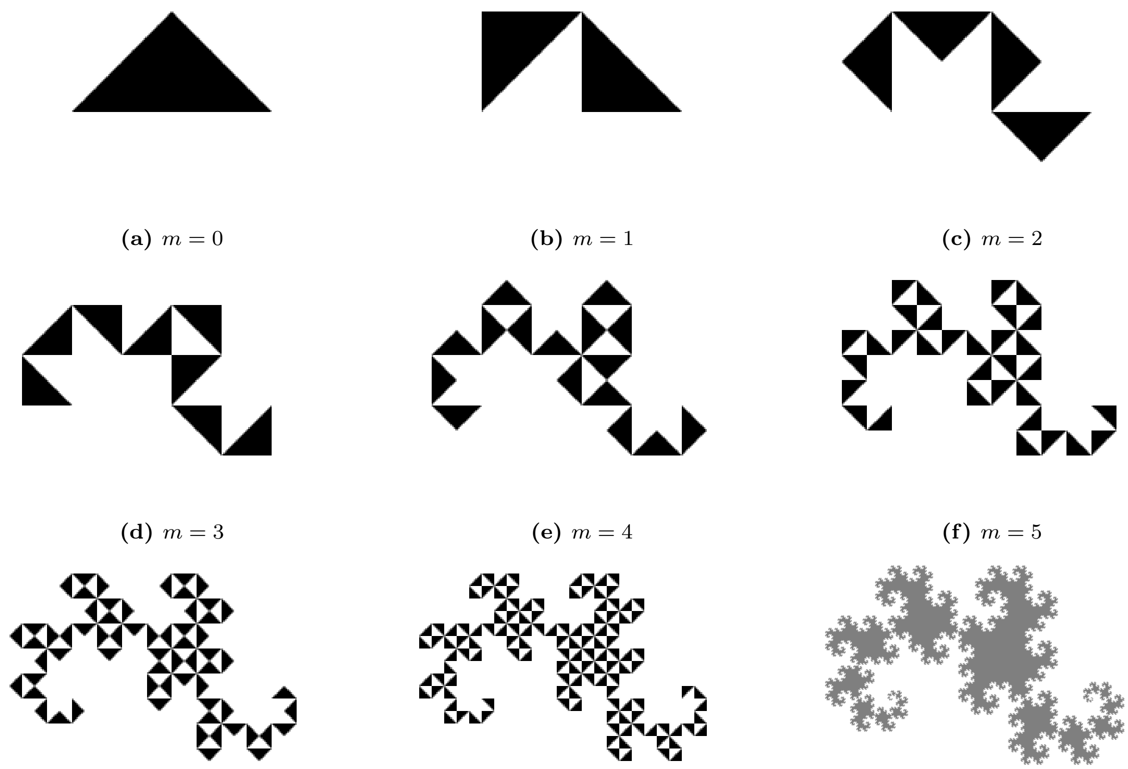

(a) $m = 0$ **(b)** $m = 1$ **(c)** $m = 2$

(d) $m = 3$ **(e)** $m = 4$ **(f)** $m = 5$

(g) $m = 6$ **(h)** $m = 7$ **(i)** $m = 20$

Figure 17: Constructing dragon curve approximations from T

The first thing to notice are visual differences between the dragon and Lévy curves. It is interesting that both fractals can be broken up into similar components which connect to neighboring components at a single point. In the Lévy curve the largest such component is the portion along the top flat edge of the curve and the rounded portion underneath. There are copies to either side rotated by $\pi/4$ and scaled down by a factor of $\sqrt{2}$. In the dragon curve these components are the solid S-shaped portions. Again, we notice that the various components are rotated by multiples of $\pi/4$ and scaled by multiples of $\sqrt{2}$.

Next we can use Equation 5 to divide the dragon curve in half as previously done in Figure 3. The result is shown in Figure 18. Notice that the largest of the components

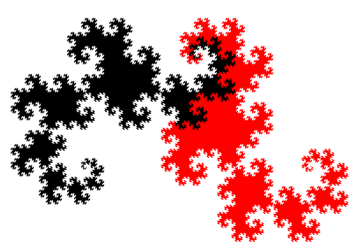

Figure 18: Dividing the dragon curve in half

described above contain both sections of F_1D and F_2D in the Lévy curve, and F_1D^* and $F_2^*D^*$ in the dragon curve. Note also that the F_1D^* does not cross $F_2^*D^*$ in the dragon curve, unlike their counterparts in the Lévy curve (both curves may achieve a point more than once, but they will not cross at this point). Since F_1D^* and $F_2^*D^*$ are also dragon curves, we can carry this on inductively and conclude that the dragon curve does not cross itself anywhere, unlike the Lévy curve.

However, Figure 17 is unsatisfying. We see that no two triangles in Figure 17 share a side, so Proposition 2 cannot apply if D^* has an interior. However, this problem is solved if we replace the triangles with squares, as shown in Figure 19.

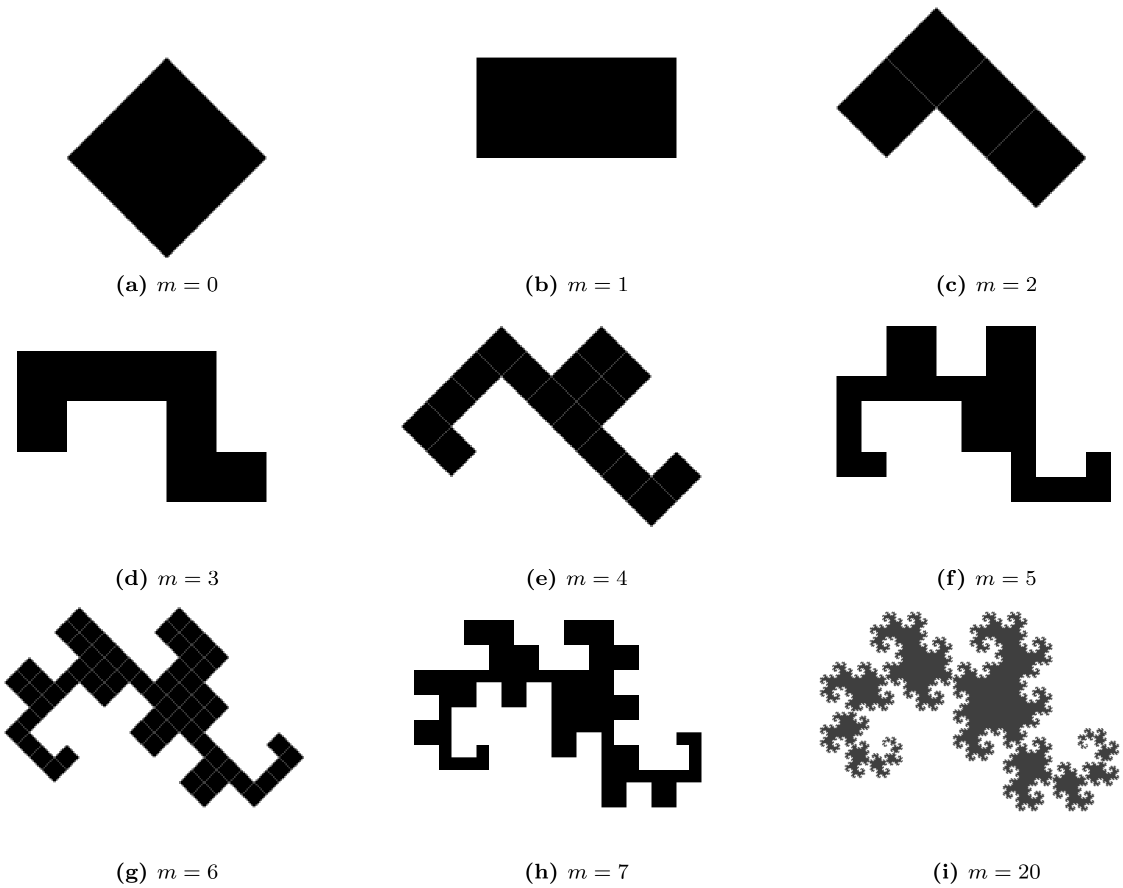

Figure 19: Constructing dragon curve approximations from squares

From this we might suspect that the dragon curve tesselates similarly to the Lévy curve. In fact, it does, as seen in Figure 20. It tesselates in the same pattern as squares (in the figure the squares would be rotated by $\pi/4$). We could logically create an analogue to Proposition 2 to find the interior of D^*, but instead of the fifteen bordering triangles, we would use the nine bordering squares. The interior of the dragon curve ends up being the large solid shapes seen in Figure 16.

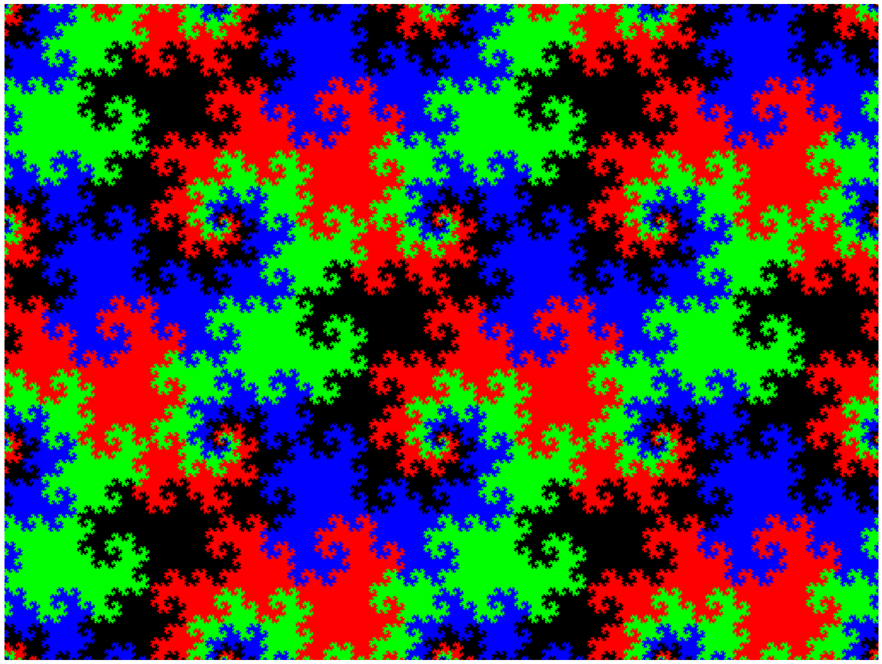

Figure 20: Tesselating the dragon curve

5 Concluding Remarks

At first glance curves such as these seem somewhat interesting and pretty, but it is not until we look a little farther that we find that there are more to them than meets the eye. With some carefully chosen approximations, we can study the interiors of these curves and find that they contain many interesting patterns and shapes, despite their simple construction.

This paper also only focused on two specific fractal curves. There are many other examples of fractals, from the simple (and related) Koch curve, to the complex and intricate Mandelbrot fractal. There are fractals that look like plants, and plants that look like fractals. We have only scratched the surface of this fascinating and beautiful area of mathematics.

A Java Code

The following is the dominant method I used to create Lévy dragons. The code uses the DrawingPanel class made by Marty Stepp, formerly of the UW CSE department. Each dragon begins at point `(x1,y1)` and ends at point `(x2,y2)`, has degree (m above) `deg`, and uses Graphics object `g`.

```
public static void levy(double x1, double y1, double x2, double y2,
                        int deg, Graphics g) {
   double midx = x1 + ((y2 - y1) + (x2 - x1)) / 2;
   double midy = y1 + ((y2 - y1) - (x2 - x1)) / 2;
   if (deg < 1) {
      Polygon poly = new Polygon();           // Creates a triangle
      poly.addPoint((int) x1,(int)  y1);      // with vertices at
      poly.addPoint((int) midx,(int)  midy); // the given points
```

```
        poly.addPoint((int) x2,(int)  y2);      //
        g.fillPolygon(poly);                    //
    } else {
        levy(x1, y1, midx, midy, deg - 1, g);   // Creates two new Levy
        levy(midx, midy, x2, y2, deg - 1, g);   // curves on these lines
    }
}
```

It is a recursive method, which reflects the self similarity of the curve. This means, when the program has to draw a Lévy cuve, it breakes it up into two smaller curves of degree `deg - 1` and draws those instead. It repeats this process until `deg = 0` when it draws a triangle.

I also wrote methods which called this one to tesselate Lévy curves and to zoom in on areas of a single curve.

Another interesting thing to note is that to change from a Lévy curve to a dragon curve one only has to change the last line of text in the code to

```
        levy(x2, y2, midx, midy, deg - 1, g);
```

B Selected Images

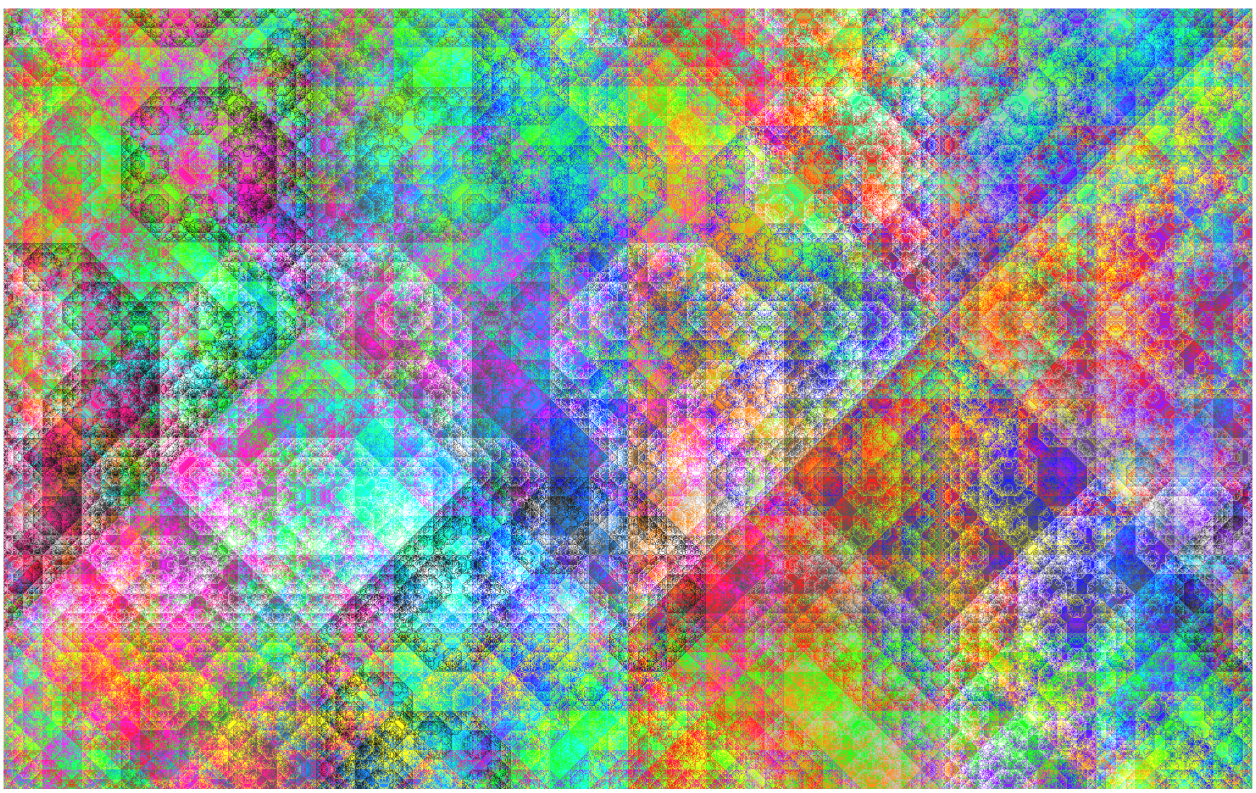

Figure 21: Tesselations of D_{20}. Each curve is about as wide as the figure is tall.

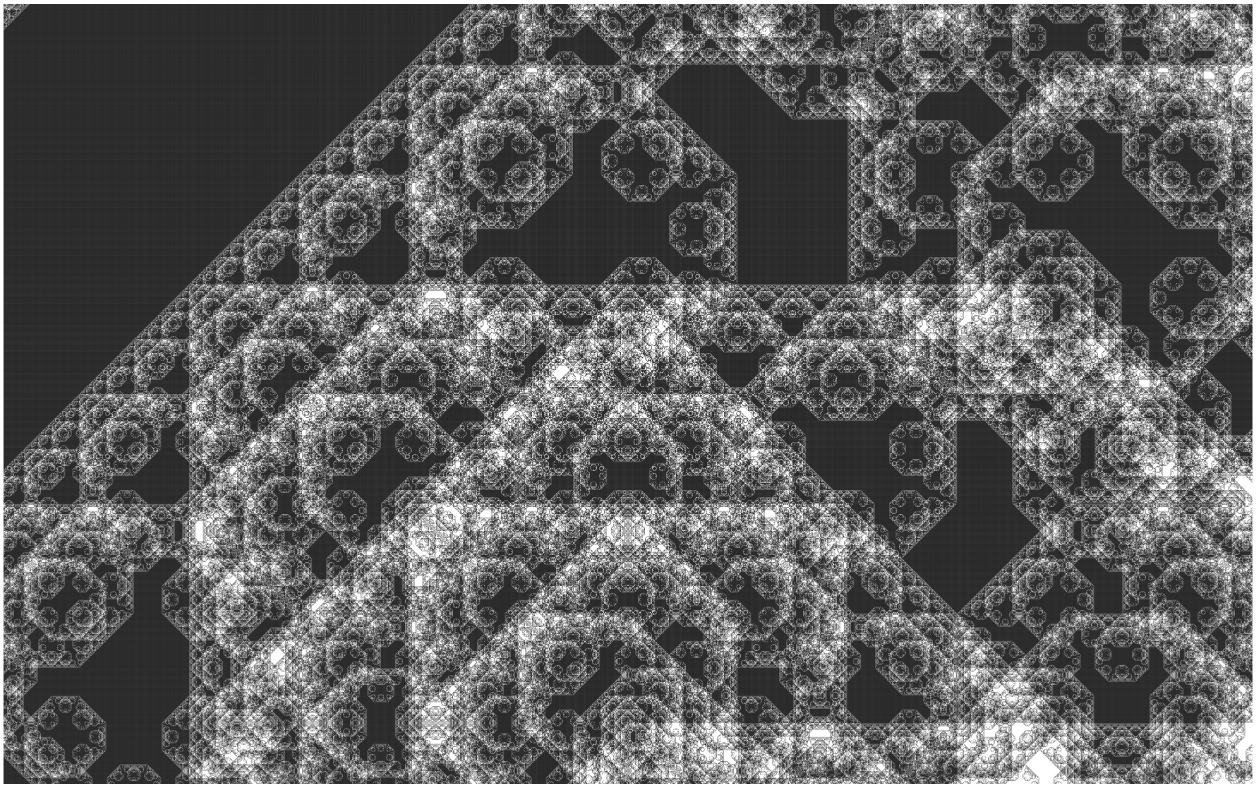

Figure 22: A close up portion of D. The dark part at the upper left is the region in Figure 10.

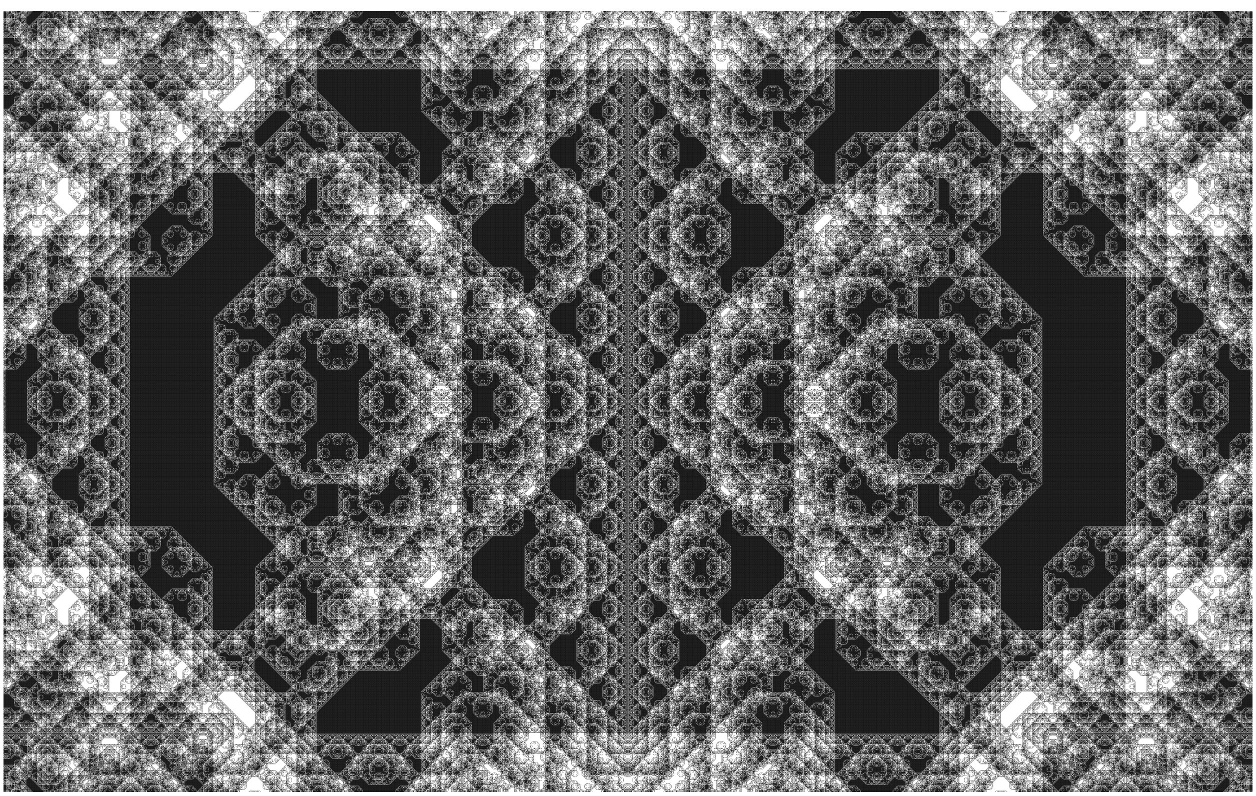

Figure 23: A close up portion of D. The center line of the image is at the center line of the curve.

References

[1] Scott Bailey, Theodore Kim, and Robert S. Strichartz. "Inside the Lévy Dragon." *American Mathematical Monthly*. Vol. 109, No. 8, October 2002, pp. 689-703.

[2] Hans Lauwerier. *Fractals: Endlessly Repeated Geometrical Figures*. Princeton University Press, Princeton, NJ, 1991.